Biochemical and Biophysical Research Communications 426 (2012) 448–453

Contents lists available at SciVerse ScienceDirect

Biochemical and Biophysical Research Communications

journal homepage: www.elsevier.com/locate/ybbrc

M-channels modulate the intrinsic excitability and synaptic responses of layer 2/3 pyramidal neurons in auditory cortex

Sujeong Lee, Jeehyun Kwag *

Department of Brain and Cognitive Engineering, Korea University, Seoul, Republic of Korea

ARTICLE INFO

Article history:
Received 4 August 2012
Available online 17 August 2012

Keywords:
M-channel
Auditory cortex
Pyramidal neuron
Spike excitability
Short-term depression

ABSTRACT

Neurons in the auditory cortex are believed to utilize temporal patterns of neural activity to accurately process auditory information but the intrinsic neuronal mechanism underlying the control of auditory neural activity is not known. The slowly activating, persistent K^+ channel, also called M-channel that belongs to the Kv7 family, is already known to be important in regulating subthreshold neural excitability and synaptic summation in neocortical and hippocampal pyramidal neurons. However, its functional role in the primary auditory cortex (A1) has never been characterized. In this study, we investigated the roles of M-channels on neuronal excitability, short-term plasticity, and synaptic summation of A1 layer 2/3 regular spiking pyramidal neurons with whole-cell current-clamp recordings *in vitro*. We found that blocking M-channels with a selective M-channel blocker, XE991, significantly increased neural excitability of A1 layer 2/3 pyramidal neurons. Furthermore, M-channels controled synaptic responses of intralaminar-evoked excitatory postsynaptic potentials (EPSPs); XE991 significantly increased EPSP amplitude, decreased the rate of short-term depression, and increased the synaptic summation. These results suggest that M-channels are involved in controlling spike output patterns and synaptic responses of A1 layer 2/3 pyramidal neurons, which would have important implications in auditory information processing.

1. Introduction

The primary auditory cortex (A1) uses temporal patterns of neural activity for auditory neural information processing [1] and disruption in temporal patterns of spikes with increased spike excitability has been observed in the case of hearing loss [2,3]. Understanding the intrinsic mechanism underlying the control of neural activity patterns of A1 neurons would shed light on how auditory information is processed. Among many intrinsic membrane channels, M-type K^+ channel (M-channel) [4], a slowly activating, non-inactivating channel belonging to the KCNQ (Kv7) family [5], has a well-established role in regulating subthreshold neural excitability in neocortical neurons of the sensory and motor cortices and the hippocampus [7–9]. It is found throughout the cortex [6] and is also known to regulate spike-frequency adaptation [7], intrinsic subthreshold resonance [10] and spike afterhyperpolarization (AHP) [10,11]. Interestingly, Kv7 has already been closely linked with auditory information processing [12], with defects in Kv7 channel subunits in cochlear [13] and central auditory pathway nuclei [14], causing hereditary hearing loss. However, the roles of M-channels in the A1 pyramidal neuronal function remains unknown.

Here, we investigated the roles of M-channels in A1 layer 2/3 pyramidal neurons' excitability, short-term plasticity, and synaptic summation *in vitro*. Using a selective M-channel blocker, XE991, we found that XE991 increases neural excitability, decreases spike-burst AHP amplitude and increases spike probability. In addition, XE991 was found to influence the rate of short-term depression (STD) and synaptic summation, suggesting that M-channels are extensively involved in controlling neural excitability and synaptic responses of A1 layer 2/3 pyramidal neurons.

2. Materials and methods

2.1. Slice preparation

All use and care of animals followed the guidelines of Institutional Animal Care and Use Committee of Korea University (KUIACUC-2011-114). After cervical dislocation and decapitation of Sprague–Dawley rats (postnatal day 21–28), the brains were rapidly removed into ice-cold, oxygenated artificial cerebrospinal fluid (ACSF) containing (in mM) NaCl, 126; KCl, 3; NaH_2PO_4, 1.25; $MgSO_4$, 2; $CaCl_2$, 2; $NaHCO_3$, 25; and glucose, 10 (pH 7.2–7.4), which was bubbled with carbogen gas (95% O_2, 5% CO_2). Coronal slices of auditory

* Corresponding author. Address: Department of Brain and Cognitive Engineering, Korea University, 145 Anam-ro, Seongbuk-gu, Seoul, Republic of Korea. Fax: +82 2 926 3268.
E-mail address: jkwag@korea.ac.kr (J. Kwag).

0006-291X/$ - see front matter © 2012 Elsevier Inc. All rights reserved.
http://dx.doi.org/10.1016/j.bbrc.2012.08.057

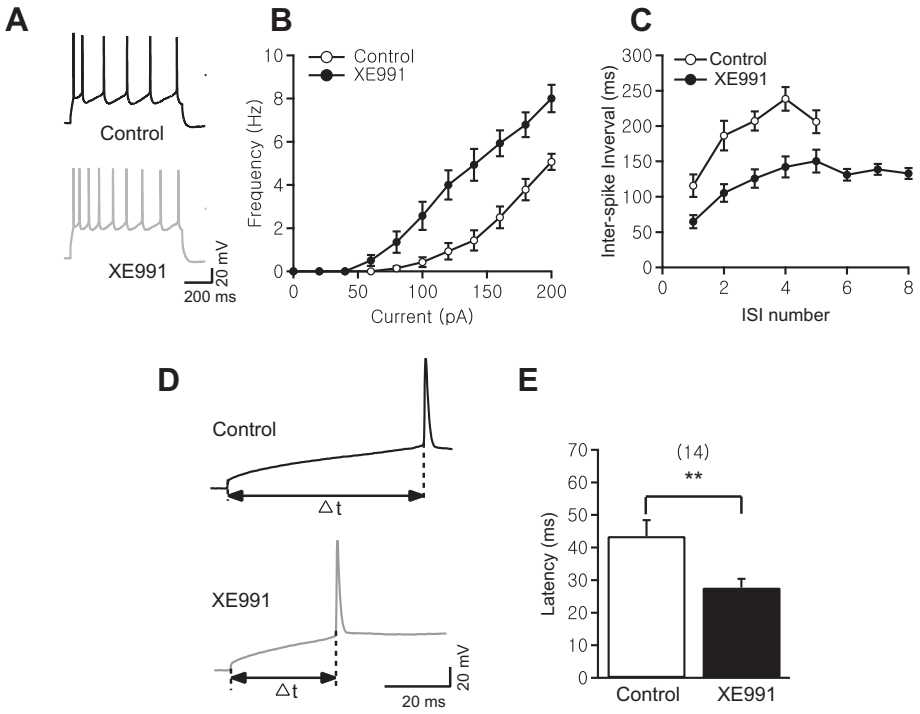

Fig. 1. M-channels modulate the intrinsic excitability of A1 layer 2/3 pyramidal neurons. (A) Voltage response of an A1 layer 2/3 pyramidal neuron to 200-pA somatic current input (1-s duration) in the control condition (black) and in the presence of XE991 (gray). (B) Frequency of spikes plotted as a function of current input amplitude (*f*–I curve) in the control condition (open circles) and in the presence of XE991 (filled circles). (C) Inter-spike interval (ISI) of A1 layer 2/3 pyramidal neurons calculated from the voltage response to 200-pA current step in the control condition (open circles) and in the presence of XE991 (filled circles). (D) Spike-onset latency of an A1 layer 2/3 pyramidal neuron subject to a 200-pA current step in the control condition (black) and in the presence of XE991 (gray). (E) Summary result of spike-onset latency in the control condition (white bar) and in the presence of XE991 (black bar). All data are mean ± SEM, $^{**}p < 0.01$, Student's *t*-test. The number of experiments is shown in parentheses.

cortex (350 μm) were cut with a vibratome (VT1000s, Leica), and slices were maintained at room temperature (22–25 °C) in a submerged-style holding chamber with oxygenated ACSF for at least 60 min before being transferred to the recording chamber perfused with oxygenated ACSF at room temperature.

2.2. Electrophysiology

Regular spiking A1 layer 2/3 pyramidal neurons were visually identified by infrared differential interference contrast video microscopy (BX51WI, Olympus). Whole-cell patch-clamp recordings were performed using a Multiclamp-700B (Molecular Devices) in current clamp-mode with patch pipettes pulled from borosilicate glass (tip resistance, 6–12 MΩ) filled with intracellular solution containing (in mM) potassium gluconate, 110; HEPES, 40; NaCl, 4; ATP–Mg, 4; and GTP, 0.3 (pH 7.2–7.3; 270–300 mOsmol/L). To block M-channel that underlies M-current (I_M), 25 μM [15,16] of the Kv7/M-channel blocker, XE991 (Tocris), was added to the ACSF. All recordings were low-pass filtered at 2 kHz and acquired at 5 kHz using ITC-18 AD board (HEKA) and Igor Pro software (Wavemetrics). Igor Pro software was used for command signal generation, data acquisition, and data analysis.

Changes in neural excitability were investigated by studying the neuronal voltage responses to current inputs (Figs. 1–3). 1-s tonic step-currents incrementing in 20-pA steps, increasing up to 200 pA, were injected into the soma to characterize the frequency–input (*f*–*I*) curve (Fig. 1A, B). Inter-spike intervals (ISIs, Fig. 1C) and spike onset-latency (Fig. 1D, E) were calculated with the voltage response to 200-pA step-current input. Spike onset-latency was calculated as the time taken for the first spike to occur in response to the current input (Fig. 1D).

To characterize the spike AHP, a single spike and spike-burst were elicited by injecting brief current pulses of 2-ms and 100-ms duration, respectively (Fig. 2). In order to study the spike probability, 50 brief current pulses (5-ms duration; 270–650 pA) were injected into the soma at 5, 10, 20, 40, 80, and 100 Hz (Fig. 3A), as has been described in Xu et al. [3]. To study the synaptic responses, a stainless steel monopolar electrode was placed in the A1 layer 2/3 region to evoke intralaminar excitatory postsynaptic potentials (EPSPs) (Fig. 4A, B). A train of 10 EPSPs were evoked at 5, 10, 20, and 40 Hz to study the effect of XE991 on STD and synaptic summation (Fig. 4C–E).

2.3. Data analysis and statistics

Neuronal membrane time constant (τ_m) and resistance (R_{in}, Table 1) were calculated by fitting an exponential curve to the early voltage response to the 40-pA hyperpolarizing current step. Spike probability was calculated as the total number of spikes evoked at each frequency divided by 50 (Fig. 3C). Peak EPSP amplitudes were normalized to the first EPSP amplitude ($EPSP_{norm}$) and a single exponential curve fit was used to estimate the decay time constant of STD (τ_{STD}, Fig. 4C) such that,

$$\mathrm{EPSP}_{\mathrm{norm}} = C_0 + C * \exp\left(\frac{-t}{\tau_{\mathrm{STD}}}\right)$$

where C_0 is the initial value and C is the amplitude constant.

The significance of differences was tested with two-sample, paired Student's *t*-tests. All data are represented as mean ± standard error of the mean (SEM).

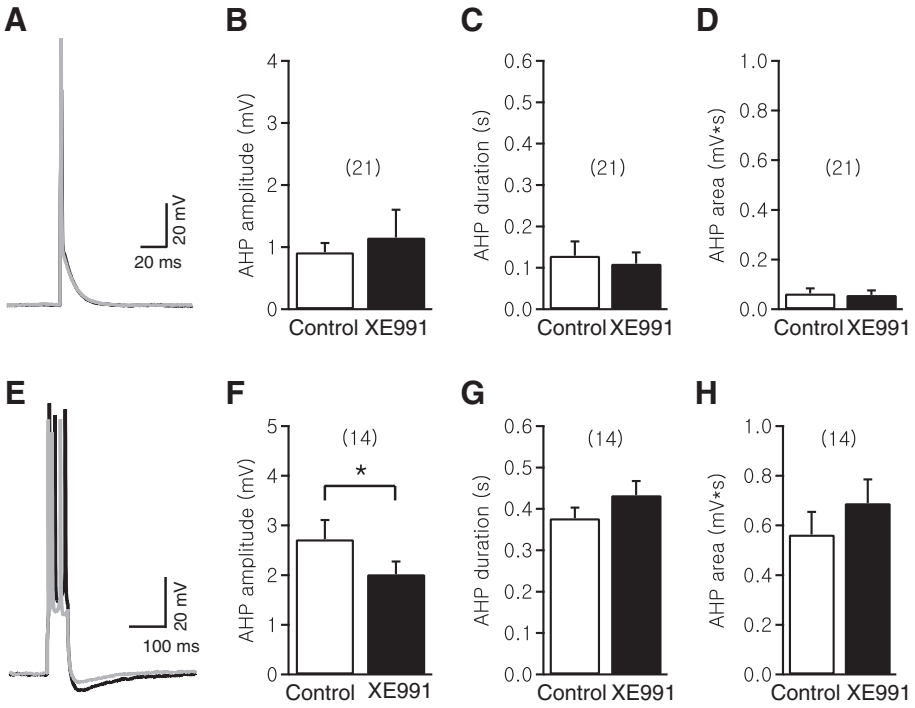

Fig. 2. M-channels modulate the after-hyperpolarizing potential (AHP) following spike-burst of A1 layer 2/3 pyramidal neurons. (A, E) A single spike (A) and a spike-burst (E) evoked in the control condition (black) and in the presence of XE991 (gray) by a brief 2-ms (A) and 100-ms (E) current pulses. (B–D) AHP amplitude, duration, and area of a single spike in the control condition (white bar) and in the presence of XE991 (black bar). (F–H) Same as in B–D but for AHP following a spike-burst. All data are mean ± SEM, $^{*}p < 0.05$, Student's *t*-test. The number of experiments is shown in parentheses.

3. Results

3.1. M-channels modulate the intrinsic excitability and spike-frquency adaptation of A1 layer 2/3 pyramidal neurons

Application of the selective M-channel blocker, XE991, significantly depolarized the A1 layer 2/3 pyramidal neuron resting membrane voltage (V_m) and increased both τ_m and R_{in} than in the control condition (Table 1, $p < 0.01$, $n = 20$). In response to 1-s depolarizing tonic step-current inputs (Fig. 1A), spike frequency increased with increasing current input amplitude in both conditions (Fig. 1B), but XE991 significantly increased the overall spike frequency for each current input amplitude (Fig. 1B, $p < 0.01$, $n = 14$). In response to 200-pA tonic current input, spike ISI increased with successive spike number showing spike-frequency adaptation in the control condition. However, spike-frequency adaptation decreased in the presence of XE991 and ISI reached a near-steady state (Fig. 1C, $n = 14$). Spike onset-latency was analyzed by calculating the time taken for the first spike to occur from the onset of the 200 pA current step (Fig. 1D) and was found to significantly shorten in the presence of XE991 than in the control condition (Fig. 1E, control: 43.5 ± 4.9 ms; XE991: 27.7 ± 2.7 ms, $p < 0.01$, $n = 14$).

3.2. M-channels modulate the spike-burst AHP of A1 layer 2/3 pyramidal neurons

Next, we assessed the effect of XE991 on AHP following a single spike and a spike-burst elicited by brief current pulses (Fig. 2A). The AHP amplitude, AHP duration, and AHP area following a single spike elicited by a 2-ms long current pulse (~1 nA) were not significantly different with or without XE991 (AHP amplitude: control = 0.92 ± 0.15 mV, XE991 = 1.15 ± 0.45 mV; AHP duration: control = 0.13 ± 0.03 s, XE991 = 0.11 ± 0.03 s; AHP area: control = 0.06 ± 0.02 mV × s, XE991 = 0.06 ± 0.02 mV × s; $n = 21$, all $p > 0.05$; Fig. 2B–D). However, AHP amplitude following a spike-burst elicited by a brief current pulse (100 ms; 500–1000 pA; Fig. 2E) significantly decreased in the presence of XE991 than in the control condition (control: 2.72 ± 0.39 mV; XE991: 2.02 ± 0.25 mV, $n = 14$, $p < 0.05$; Fig. 2F). However, neither AHP duration nor area following a spike-burst were significantly different (AHP duration: control = 0.38 ± 0.03 ms, XE991 = 0.43 ± 0.03 ms, $n = 14$, $p > 0.05$; AHP area: control = 0.56 ± 0.09 mV × s, XE991 = 0.69 ± 0.09 mV × s, $n = 14$, $p > 0.05$; Fig. 2G, H).

3.3. XE991 increases spike probability of A1 layer 2/3 pyramidal neurons

To determine whether M-channels influence the discharge patterns of A1 layer 2/3 pyramidal neurons subject to different input frequencies, 50 trains of brief, depolarizing current pulses were given at 5, 20, 40, 60, 80, and 100 Hz (Fig. 3A). The pulse amplitude was adjusted at the beginning of each experiment so that spikes were evoked for every pulse at 5 Hz in the control condition and this was kept constant for all stimulus frequencies throughout the experiments. Spike number decreased as stimulus frequency increased (Fig. 3A, B). Spike probability, calculated as the number of spikes divided by the number of current pulses (50, Fig. 3C), increased in the presence of XE991 compared to the control condition (20 Hz: control = 0.78 ± 0.04, XE991 = 0.96 ± 0.02; 40 Hz: control = 0.71 ± 0.02, XE991 = 0.90 ± 0.03; 60 Hz: control = 0.54 ± 0.04, XE991 = 0.54 ± 0.02; 80 Hz: control: 0.45 ± 0.04, XE991: 0.49 ± 0.03; 100 Hz: control = 0.34 ± ± 0.04, XE991: 0.36 ± 0.02, $n = 14$; Fig. 3C). However, spike probability significantly increased only at 20 and 40 Hz ($n = 14$, $p < 0.01$; Fig. 3C).

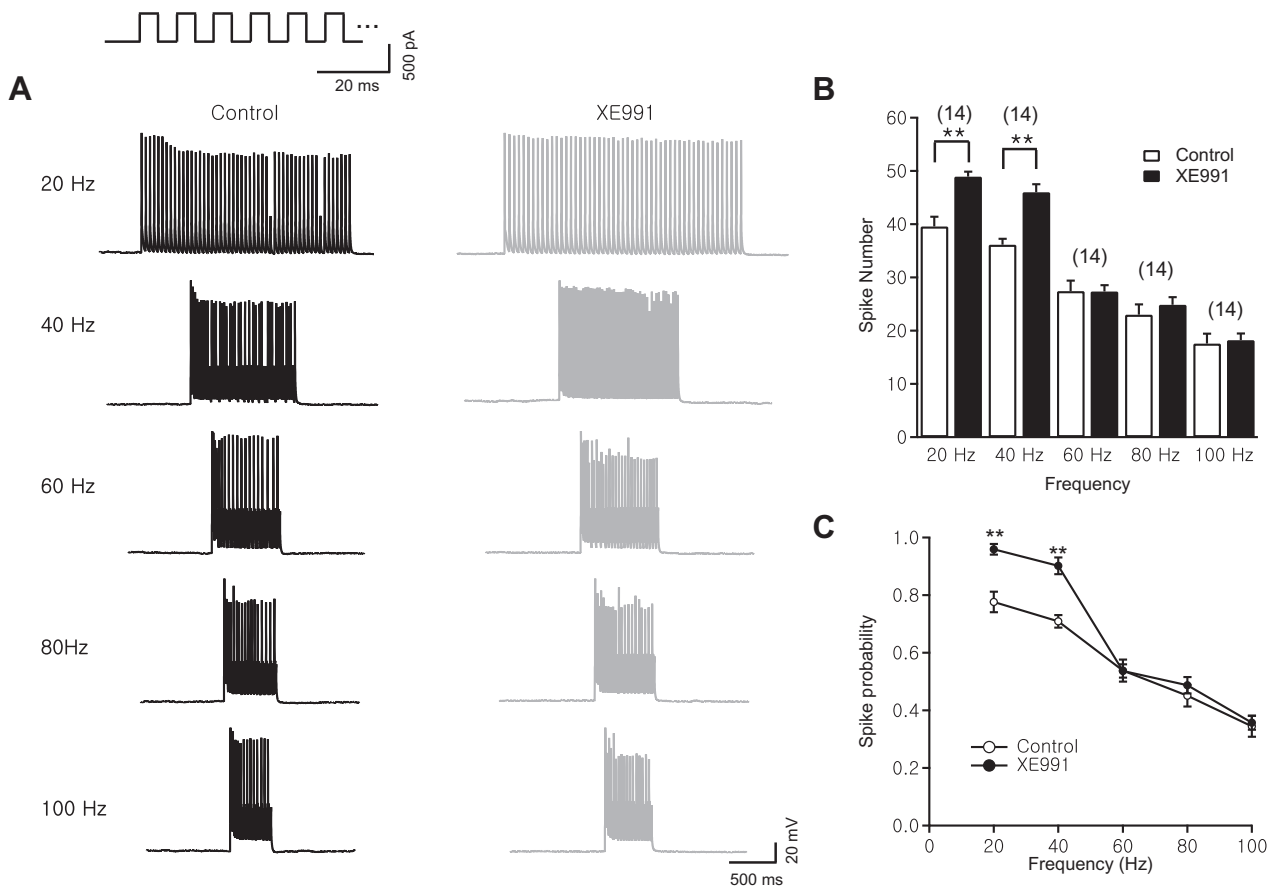

Fig. 3. Modulation of spike probability of A1 layer 2/3 pyramidal neurons by M-channels. (A) Top, a schematic of a train of current pulses (5-ms duration) injected at the soma at 100 Hz. The corresponding voltage response to 20, 40, 60, 80, and 100 Hz of current pulses in the control condition (left, black) and in the presence of XE991 (right, gray). (B) Number of spikes elicited at each frequency in the control condition (white bar) and in the presence of XE991 (black bar). (C) Spike probability plotted against the input frequencies. All data are mean ± SEM, $^{**}p < 0.01$, Student's *t*-test. The number of experiments is shown in parentheses.

3.4. The effect of M-channels on intralaminar-evoked EPSPs, short-term depression, and synaptic summation of A1 layer 2/3 pyramidal neurons

Finally, we investigated the roles of M-channels on synaptic responses evoked by intralaminar synaptic stimulation of A1 layer 2/3 region. The amplitude of a single EPSP evoked in the presence of XE991 was larger than that in the control condition (Fig. 4A, left). When the EPSP amplitude with XE991 was normalized to that of the control condition, it was significantly larger than that in the control condition (control: 1.00 ± 0.07, XE991 = 1.28 ± 0.12, $n = 13$, $p < 0.05$; Fig. 4A, right).

STD has been widely observed in the A1 layer 2/3 region and has been implicated in regulating adaptive responses during auditory information processing [17,18]. Consistent with previous reports [19,20], a train of 10 synaptic stimulations evoked at 5, 10, 20, and 40 Hz resulted in STD at all frequencies in both conditions (Fig. 4B). The time constant of STD, τ_{STD}, was shorter in the control condition than in the presence of XE991 across all frequencies (5 Hz: control = 477.7 ms, XE991 = 732.4 ms; 10 Hz: control = 265.2 ms, XE991 = 443.4 ms; 20 Hz: control = 150.5 ms, XE991 = 215.2 ms; 40 Hz: control = 40.0 ms, XE991 = 51.7 ms, solid lines are exponential fit; Fig. 4C). The EPSP ratio of the first EPSP ($EPSP_1$) and the tenth EPSP ($EPSP_{10}$) ($EPSP_{10}/EPSP_1$) in the presence of XE991 was significantly larger for all frequencies (5 Hz: control = 0.61 ± 0.05, XE991 = 0.70 ± 0.05; 10 Hz: control = 0.45 ± 0.06, XE991 = 0.57 ± 0.06; 20 Hz: control = 0.30 ± 0.04, XE991 = 0.39 ± 0.05; all $p < 0.01$, n = 13; Fig. 4D) except at 40 Hz (control = 0.19 ± 0.03, XE991 = 0.23 ± 0.05; $p > 0.05$, $n = 13$; Fig. 4D).

To study the role of M-channels in synaptic summation, the area under the train of 10 EPSPs evoked at each frequency was quantified (Fig. 4E). As previously observed in hippocampal neurons [9], XE991 increased the area of EPSPs at all tested frequencies. However, the increase was only statistically significant at 5 Hz (control = 1.17 ± 0.20 mV × s, XE991 = 1.81 ± 0.31 mV × s, $p < 0.05$, $n = = 13$; Fig. 4E) but there was no significant differences at higher frequencies (10 Hz: control = 1.04 ± 0.16 mV × s, XE991 = 1.43 ± 0.31 mV × s, 20 Hz: control = 0.84 ± 0.11 mV × s, XE991 = 1.06 ± 0.18 mV × s, 40 Hz: control = 0.51 ± 0.07 mV × s, XE991 = 0.61 ± 0.11 mV × s, $p > 0.05$, $n = 13$; Fig. 4E). These results indicate that M-channels modulate EPSP amplitude, STD, and synaptic summation of A1 layer 2/3 pyramidal neurons.

4. Discussion

Our results demonstrate the roles of M-channels on neural excitability and synaptic responses in regular spiking A1 layer 2/3 pyramidal neurons *in vitro*. Blocking M-channels with XE991 increased neural excitability and spike probability, whereas it decreased spike-onset latency and spike-frequency adaptation. These alterations in intrinsic excitability were accompanied by changes in spike-burst AHP where XE991 decreased AHP amplitude. M-channels also modulated STD and synaptic summation of layer 2/3 synapses; XE991 decreased the rate of STD and enhanced synaptic summation. Modulation of neural excitability, STD, and synaptic summation by M-channels suggests that M-channels might have important functions in auditory information processing.

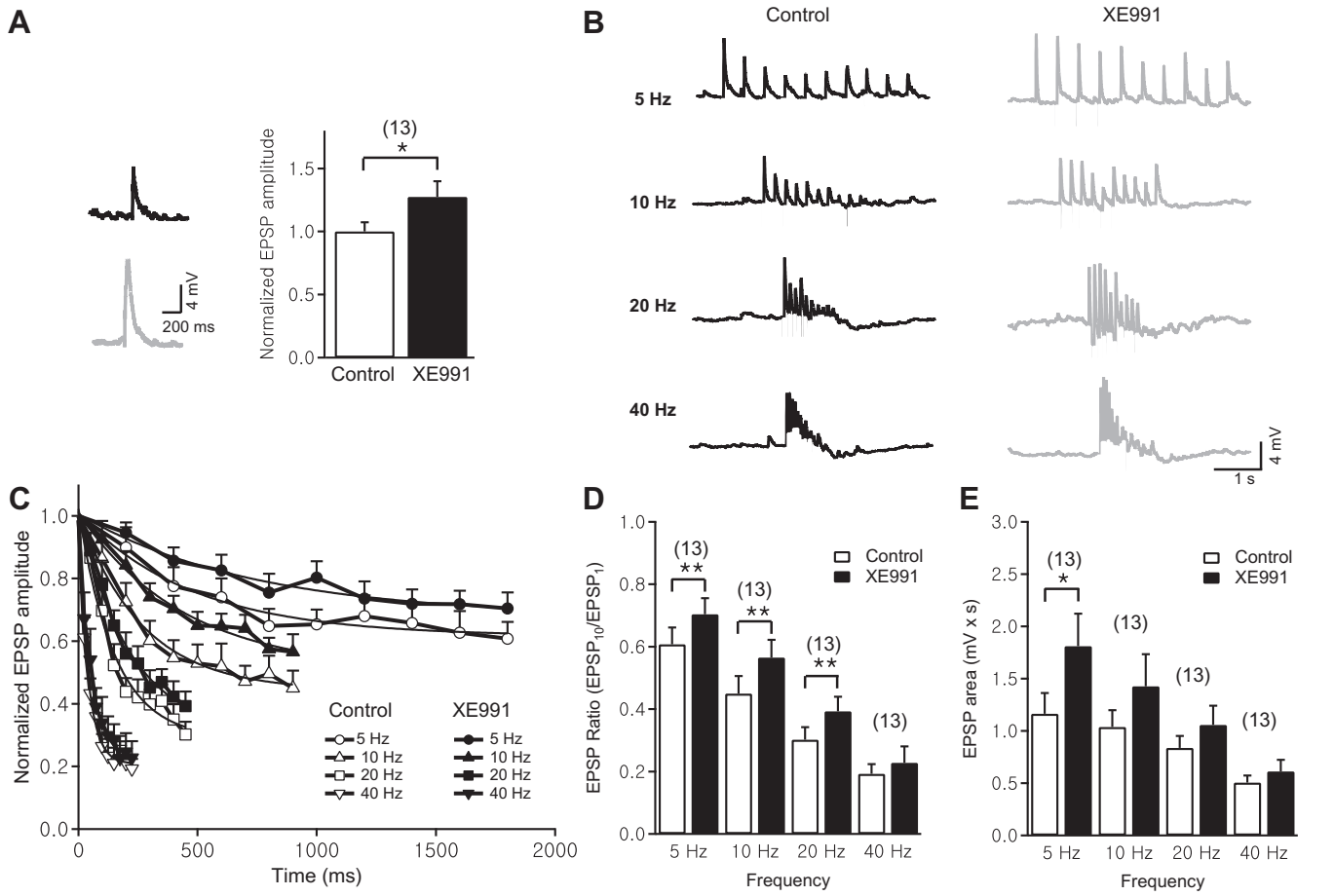

Fig. 4. The effect of XE991 on excitatory postsynaptic potential (EPSP), short-term depression (STD), and EPSP summation of A1 layer 2/3 pyramidal neurons. (A) Left, an example voltage trace of an intralaminar-evoked single EPSP in A1 layer 2/3 in the control condition (black) and in the presence of XE991 (gray). Right, EPSP amplitude in the control condition (white bar) and in the presence of XE991 (black bar) normalized to the EPSP amplitude in the control condition. (B) A train of 10 EPSPs evoked in A1 layer 2/3 at 20, 40, 60, 80, and 100 Hz, in the control condition (left, black) and in the presence of XE991 (right, gray) to test STD. (C) A train of 10 EPSPs amplitudes normalized to the first EPSP amplitude ($EPSP_1$) and plotted against the inter-stimulus interval. Solid lines indicate the exponential fit to the plot. (D) EPSP ratio ($EPSP_{10}/EPSP_1$) calculated as the 10th EPSP amplitude ($EPSP_{10}$) divided by $EPSP_1$ plotted at each frequency. (E) Area of a train of 10 EPSPs evoked at different frequencies in the control condition (white bar) and in the presence of XE991 (black bar) to test EPSP summation. All data are mean ± SEM, $^{*}p < 0.05$, $^{**}p < 0.01$, Student's *t*-test. The number of experiments is shown in parentheses.

Table 1
The effect of XE991 on membrane properties of A1 layer 2/3 pyramidal neurons. Resting membrane potential (V_m), input resistance (R_{in}), and time constant (τ_m) of A1 layer 2/3 pyramidal neurons in the control condition and in the presence of XE991 ($n = 20$). All data are mean ± SEM, $^{**}p < 0.01$, Student's *t*-test.

	Resting membrane potential (V_m, mV)	Input resistance (R_{in}, MΩ)	Time constant (τ_m, ms)
Control	−69.4 ± 0.9**	106.5 ± 4.7**	20.0 ± 1.6**
XE991	−67.0 ± 0.9	149.6 ± 9.6	34.5 ± 2.8

A1 layer 2/3 pyramidal neurons are reported to exhibit spike-frequency adaptation in response to constant [21] and repetitive depolarizing current inputs [22]. Spike-frequency adaptation was recently shown to partly be mediated by K^+, Ca^{2+}-activated K^+ and Na^+-activated K^+ channels [21,22]. However, blocking these K^+ channels did not completely remove spike-frequency adaptation [21]. In our study, XE991 was found to decrease spike-frequency adaptation (Fig. 1A, C), which suggests that it is the M-channels that underlie the remainder of the adaptive current in A1 layer 2/3 pyramidal neurons. Blocking M-channels significantly increased spike excitability (Fig. 1B) and the spike probability (Fig. 3). These changes in intrinsic excitability might be due to alterations in neuronal membrane property, as well as spike shape. Indeed, XE991 significantly depolarized V_m and increased both τ_m and R_{in} (Table 1). Increased excitability could also be due to alterations in the AHP during and after repetitive spike discharges [10,11,23] because XE991 significantly reduced the spike-burst AHP amplitude (Fig. 2E, F). These changes of intrinsic neuronal properties following M-channel modulation are similar to those observed in sensory and motor cortical neurons [8], entorhinal cortex [24], and the hippocampus [7,9–11]. Thus, the presence of M-channels in A1 layer 2/3 pyramidal neurons may also serve as an intrinsic mechanism that stabilizes neuronal membrane properties and neural firing, which may be important for accurate auditory processing [1].

Activity-dependent changes in intrinsic properties occur in cortical and hippocampal neurons to control spike pattern and frequency [25–27], which are vital for neural computation [1,27]. Although these changes have not been demonstrated in the A1 yet, Kv7 channel expression is known to increase in an activity-dependent manner [27]. A decrease in sound-driven neural activity reaching the auditory cortex, such as in the case of sensorineural hearing loss (SNHL) and conductance hearing loss (CHL) [2,3], could potentially interfere with activity-dependent Kv7 modulation and consequently alter A1 spike output patterns. Indeed, K^+ channels have already been suggested as a possible candidate underlying development-related changes in subthreshold intrinsic

properties [19] in cochlear, auditory brain stem, and cortical neurons [28–30]. The number of KCNQ channels is known to increase with development [31]. Also, layer 2/3 pyramidal neurons in SNHL and CHL show increased neural excitability and spike probability, similar to the activity we observed following Kv7 blockade (Figs. 1–3). Thus, an attractive hypothesis to be tested in the future is to assess Kv7 modulation in the A1 in animal models of hearing loss and in Kv7 knock-out mice [32].

We demonstrated that XE991 increases EPSP amplitude, consistent with the observations in hippocampal CA1 pyramidal neurons [33]. STD was observed at all tested frequencies in both conditions (Fig. 4B–D) and the rate of STD decreased in the presence of XE991 compared to the control condition (Fig. 4C). STD is believed to be mostly mediated by a presynaptic mechanism where the release probability decreases with repetitive stimuli [34]. However, M-channels are present in both presynaptic and postsynaptic locations [35]. Therefore, it would be interesting to find out the synaptic location of M-channels involved in the modulation of STD in future experiments. XE991 also enhanced synaptic summation of A1 layer 2/3 pyramidal neurons, where the summated EPSP area in the presence of XE991 significantly increased relative to the control condition at 5 Hz (Fig. 4E). Because EPSP summation is known to decrease with development [19], it would be interesting to test whether developmental changes modulate Kv7 expression and function.

In conclusion, we show the M-channels can control neural excitability and synaptic responses of A1 layer 2/3 pyramidal neurons. Impaired neuronal firing patterns may be a central issue in dysfunctional auditory processing observed with hearing loss and, on the basis of the known therapeutic potentials of the Kv7 channels [36], M-channel could play an important role in understanding the mechanisms underlying hearing loss as well as auditory information processing.

Acknowledgments

This work was supported by the World Class University (WCU) program (R31-10008) and by the Basic Science Research Program (2012-0003500) through the National Research Foundation of Korea funded by the Ministry of Education, Science, and Technology.

References

[1] X. Wang, Neural coding strategies in auditory cortex, Hear. Res. 229 (2007) 81–93.
[2] V.C. Kotak, S. Fujisawa, F.A. Lee, O. Karthikeyan, C. Aoki, D.H. Sanes, Hearing loss raises excitability in the auditory cortex, J. Neurosci. 25 (2005) 3908–3918.
[3] H. Xu, V.C. Kotak, D.H. Sanes, Conductive hearing loss disrupts synaptic and spike adaptation in developing auditory cortex, J. Neurosci. 27 (2007) 9417–9426.
[4] D.A. Brown, P.R. Adams, Muscarinic suppression of a novel voltage-sensitive K+ current in a vertebrate neurone, Nature 283 (1980) 673–676.
[5] D.A. Brown, G.M. Passmore, Neural KCNQ (Kv7) channels, Br. J. Pharmacol. 156 (2009) 1185–1195.
[6] J.J. Devaux, K.A. Kleopa, E.C. Cooper, S.S. Scherer, KCNQ2 is a nodal K+ channel, J. Neurosci. 24 (2004) 1236–1244.
[7] S.P. Aiken, B.J. Lampe, P.A. Murphy, B.S. Brown, Reduction of spike frequency adaptation and blockade of M-current in rat CA1 pyramidal neurones by linopirdine (DuP 996), a neurotransmitter release enhancer, Br. J. Pharmacol. 115 (1995) 1163–1168.
[8] D. Guan, M.H. Higgs, L.R. Horton, W.J. Spain, R.C. Foehring, Contributions of Kv7-mediated potassium current to sub- and suprathreshold responses of rat layer II/III neocortical pyramidal neurons, J. Neurophysiol. 106 (2011) 1722–1733.
[9] H. Hu, K. Vervaeke, J.F. Storm, M-channels (Kv7/KCNQ channels) that regulate synaptic integration, excitability, and spike pattern of CA1 pyramidal cells are located in the perisomatic region, J. Neurosci. 27 (2007) 1853–1867.
[10] C. Yue, Y. Yaari, KCNQ/M channels control spike after depolarization and burst generation in hippocampal neurons, J. Neurosci. 24 (2004) 4614–4624.
[11] N. Gu, K. Vervaeke, H. Hu, J.F. Storm, Kv7/KCNQ/M and HCN/h, but not KCa2/SK channels, contribute to the somatic medium after-hyperpolarization and excitability control in CA1 hippocampal pyramidal cells, J. Physiol. 566 (2005) 689–715.
[12] M.R. Brown, L.K. Kaczmarek, Potassium channel modulation and auditory processing, Hear. Res. 279 (2011) 32–42.
[13] C. Kubisch, B.C. Schroeder, T. Friedrich, B. Lutjohann, A. El-Amraoui, S. Marlin, C. Petit, T.J. Jentsch, KCNQ4, a novel potassium channel expressed in sensory outer hair cells, is mutated in dominant deafness, Cell 96 (1999) 437–446.
[14] T. Kharkovets, J.P. Hardelin, S. Safieddine, M. Schweizer, A. El-Amraoui, C. Petit, T.J. Jentsch, KCNQ4, a K+ channel mutated in a form of dominant deafness, is expressed in the inner ear and the central auditory pathway, Proc. Natl. Acad. Sci. USA 97 (2000) 4333–4338.
[15] M.S. Grubb, J. Burrone, Channelrhodopsin-2 localised to the axon initial segment, PLoS One 5 (2010) e13761.
[16] R.H. Pineda, A.B. Ribera, Dorsal-ventral gradient for neuronal plasticity in the embryonic spinal cord, J. Neurosci. 28 (2008) 3824–3834.
[17] A.M. Oswald, M.L. Schiff, A.D. Reyes, Synaptic mechanisms underlying auditory processing, Curr. Opin. Neurobiol. 16 (2006) 371–376.
[18] A.D. Reyes, Synaptic short-term plasticity in auditory cortical circuits, Hear. Res. 279 (2011) 60–66.
[19] A.M. Oswald, A.D. Reyes, Maturation of intrinsic and synaptic properties of layer 2/3 pyramidal neurons in mouse auditory cortex, J. Neurophysiol. 99 (2008) 2998–3008.
[20] M. Atzori, S. Lei, D.I. Evans, P.O. Kanold, E. Phillips-Tansey, O. McIntyre, C.J. McBain, Differential synaptic processing separates stationary from transient inputs to the auditory cortex, Nat. Neurosci. 4 (2001) 1230–1237.
[21] S. Huggenberger, M. Vater, R.A. Deisz, Interlaminar differences of intrinsic properties of pyramidal neurons in the auditory cortex of mice, Cereb. Cortex 19 (2009) 1008–1018.
[22] J.M. Abolafia, R. Vergara, M.M. Arnold, R. Reig, M.V. Sanchez-Vives, Cortical auditory adaptation in the awake rat and the role of potassium currents, Cereb. Cortex 21 (2011) 977–990.
[23] J.F. Storm, An after-hyperpolarization of medium duration in rat hippocampal pyramidal cells, J. Physiol. 409 (1989) 171–190.
[24] M. Yoshida, A. Alonso, Cell-type specific modulation of intrinsic firing properties and subthreshold membrane oscillations by the M(Kv7)-current in neurons of the entorhinal cortex, J. Neurophysiol. 98 (2007) 2779–2794.
[25] R.H. Cudmore, G.G. Turrigiano, Long-term potentiation of intrinsic excitability in LV visual cortical neurons, J. Neurophysiol. 92 (2004) 341–348.
[26] H. Misonou, D.P. Mohapatra, E.W. Park, V. Leung, D. Zhen, K. Misonou, A.E. Anderson, J.S. Trimmer, Regulation of ion channel localization and phosphorylation by neuronal activity, Nat. Neurosci. 7 (2004) 711–718.
[27] W.W. Wu, C.S. Chan, D.J. Surmeier, J.F. Disterhoft, Coupling of L-type Ca2+ channels to KV7/KCNQ channels creates a novel, activity-dependent, homeostatic intrinsic plasticity, J. Neurophysiol. 100 (2008) 1897–1908.
[28] J. Kang, J.R. Huguenard, D.A. Prince, Development of BK channels in neocortical pyramidal neurons, J. Neurophysiol. 76 (1996) 188–198.
[29] R. Kanjhan, C.L. Balke, G.D. Housley, M.C. Bellingham, P.G. Noakes, Developmental expression of two-pore domain K+ channels, TASK-1 and TREK-1, in the rat cochlea, Neuroreport 15 (2004) 437–441.
[30] Y. Nakamura, T. Takahashi, Developmental changes in potassium currents at the rat calyx of Held presynaptic terminal, J. Physiol. 581 (2007) 1101–1112.
[31] N. Tinel, I. Lauritzen, C. Chouabe, M. Lazdunski, M. Borsotto, The KCNQ2 potassium channel: splice variants, functional and developmental expression. Brain localization and comparison with KCNQ3, FEBS Lett. 438 (1998) 171–176.
[32] T.J. Jentsch, Neuronal KCNQ potassium channels: physiology and role in disease, Nat. Rev. Neurosci. 1 (2000) 21–30.
[33] M.M. Shah, M. Migliore, D.A. Brown, Differential effects of Kv7 (M-) channels on synaptic integration in distinct subcellular compartments of rat hippocampal pyramidal neurons, J. Physiol. 589 (2011) 6029–6038.
[34] R.S. Zucker, W.G. Regehr, Short-term synaptic plasticity, Annu. Rev. Physiol. 64 (2002) 355–405.
[35] A. Peretz, A. Sheinin, C. Yue, N. Degani-Katzav, G. Gibor, R. Nachman, A. Gopin, E. Tam, D. Shabat, Y. Yaari, B. Attali, Pre- and postsynaptic activation of M-channels by a novel opener dampens neuronal firing and transmitter release, J. Neurophysiol. 97 (2007) 283–295.
[36] V.K. Gribkoff, The therapeutic potential of neuronal KCNQ channel modulators, Expert Opin. Ther. Targets 7 (2003) 737–748.